Near surface velocity estimation using early-arrival waveform inversion constrained by residual statics

Xukai Shen

ABSTRACT

Early-arrival waveform inversions estimate near-surface velocity by matching the modeled and observed waveforms. Velocity estimated by such inversion usually has higher resolution if higher-frequency parts of early arrivals are used and data are surfficiently sampled in space. However, for land data, early arrivals usually contain more noise at higher frequencies, which makes higher-frequency data less reliable for waveform matching, also sampling is usually sparse due to cost considerations. Surface-consistent residual statics can correct the traveltime perturbations of deeper reflections caused by small near-surface velocity heterogeneities, assuming that rays travel vertically through the near-surface. Under this assumption, residual statics can provide information about small velocity heterogeneities. In this paper, I formulate the near-surface velocity estimation problem by constraining early-arrival waveform inversion with a modified version of receiver residual statics. The synthetic result shows that for inversion of early arrivals with relatively low frequency content, velocity estimation constrained by residual statics can provide a more detailed near-surface velocity field and more consistent reflector locations across migrated images from different shots.

INTRODUCTION

Near-surface velocity can be important for imaging deeper reflectors. The conventional ways of estimating near-surface velocity are refraction statics (Hampson and Russell, 1984; Olson, 1984) and turning-ray tomography (White, 1989). These methods pick first breaks, and then iteratively estimate the near-surface velocity model by tracing rays through it and minimizing the difference between modeled first breaks and picked first breaks. Waveform inversion, a more sophisticated method, tries to match the waveform rather than the first-break traveltimes (Tarantola, 1984; Pratt and Hicks, 1998; Mora, 1987). By matching the waveform, more information in the data is used, resulting in higher resolution of the estimated velocity. When the higher-frequency parts of data are used, the estimated velocity usually has higher resolution (Sirgue and Pratt, 2004). Recently, people have applied this idea to estimate near-surface velocity by matching the refracted arrivals (C. Ravaut and Dell'Aversana, 2004) or early arrivals in general (J. Sheng and Schuster, 2006), while both papers use velocity estimated from refraction statics as the initial solution. Both these papers

report higher resolution of estimated velocity after early-arrival waveform inversion and better migrated images using the estimated velocity. However, early arrivals in land data are usually very noisy at higher frequencies. Matching data in the presence of such noise is difficult and is likely to introduce errors in estimated velocity. Another important factor that affects the resolution of waveform inversion is receiver sampling. If receiver sampling is dense enough, then the wavefield perturbation caused by small scale velocity anomalies will be observed and can be used to invert for these small scale velocity features. Otherwise, these small perturbations are missing and result in lower resolution of estimated velocity. To obtain high-resolution velocity without using noisy high-frequency data and in the absence of densely sampled receiver data, I propose to use the receiver residual statics differences as a constraint in the early-arrival waveform inversion.

I define receiver residual-statics difference (RRSD) as the static shift between adjacent traces within the same shot. There are two ways of obtaining such measurements, one is to measure it from all shot gathers, and for each receiver location, such measured RRSDs are usually not exactly the same across different shots; the other way is to calculate it from near surface velocity using the surface-consistent concept. The surface-consistency concept is built on the assumption that rays reflected from deep reflectors travel vertically in the near surface. Conventional residual statics methods use the concept to derive surface-consistent receiver/source residual statics for each receiver/source location. The two kind of RRSDs defined here share some similarities with the conventional residual statics. The measured RRSDs from all shot gathers are not surface-consistent, however, they quantitatively show how reflection events in each shots are affected by near surface velocity anomalies. The modeled RRSDs from near surface velocities are derived from near-surface velocity, and thus are surface-consistent, but they are not so closely related to reflection events in recorded data. By forcing certain similarities between the modeled RRSDs and measured RRSDs, the vertically traveling ray assumption can be used to connect near-surface velocity and measured RRSDs analytically. Many authors (Rothman, 1985; Ronen and Claerbout, 1985) have noticed similarity between the results of conventional surface-consistent residual-statics estimations and the structures of near-surface velocity anomalies . In the case of RRSD, these similarities reflect the traveltime difference of vertical rays at adjacent receiver locations. By forcing similarities between the measured RRSDs and modeled RRSDs in the least square sense, discrete time sampling of modeled RRSDs from near surface velocity can be avoided. On the other hand, if conventional residual statics are used here, such traveltime differences between each pair of adjacent traces become discrete, which are usually not realistic.

The paper is organized as follows: I first set up the inverse problem mathematically with both waveform fitting goals and RRSD fitting goals. I then test the algorithm on a synthetic example. Last, I conclude with possible improvements and future directions.

THEORY

The overall fitting goal can be written as

$$\begin{cases} \mathbf{W_e F_{bp}} \left(\mathbf{D(m)} - \mathbf{d_{obs}}\right) \approx \mathbf{0} \\ \epsilon \left(\mathbf{T(m)} - \delta\tau_{\mathbf{obs}}\right) \approx \mathbf{0} \end{cases} \tag{1}$$

where $\mathbf{m}$ is the model, which consists of near-surface slowness (inverse of near surface velocity); $\mathbf{d_{obs}}$ are data, which consist of the recorded wavefield; $\mathbf{W_e}$ is a weighting function that windows out early arrivals; $\mathbf{F_{bp}}$ is the bandpass operator to selectively use the different frequency content of recorded early arrivals; $\mathbf{D}$ is the constant-density two-way acoustic wave-equation operator that generates synthetic early arrivals from source and near-surface velocity; and $\delta\tau_{\mathbf{obs}}$ is the measured RRSD from all shot and receiver locations. $\mathbf{T}$ is the operator that calculates RRSD, assuming vertically traveling rays in the near surface; and ϵ is a number that balances the relative weighting of the two fitting goals, since the data in these equations are in different spaces and the first equation is the the major fitting goal. In the synthetic example shown here, I do not estimate the source wavelet, and source wavelet estimation will be added later. Next I will describe each fitting goal in more detail

Waveform inversion has been extensively studied, and there are many references on how to implement the algorithm (Mora, 1987; Tarantola, 1984; Pratt and Hicks, 1998). To match early arrivals, the only additional difference is the weighting of both recorded data and modeled data. The weighting acts as a window that mutes anything that is not an early arrival. In addition, to selectively use the different frequency content of recorded early arrivals, both recorded data and synthetic data will be band passed before applying the weighting function. Since the objective function of waveform inversion is more linear with respect to velocity at lower frequencies. The waveform inversion I use is a time-domain method, where all the wave propagation is done in the time domain, using an explicit finite-difference scheme with 6th order accuracy in space and 2nd order accuracy in time.

The second fitting goal in equation 1 is to minimize the misfit between the modeled RRSD and measured RRSD. Notice that for each receiver location, there is only one modeled RRSD, which is modeled from near-surface velocity assuming vertically traveling rays. On the other hand, there are many measured RRSD at each receiver location; the number of measurements equals the number of shots that were recorded at that receiver location. By having many measurements at each receiver location, the fitting goal is more robust in the presence of potentially biasing noise. The current algorithm minimizes the misfit in the least-square sense. I model the RRSD in two steps: first I calculate the traveltime of vertical rays through near-surface velocity; then I take the difference of all these modeled RRSDs along the receiver axis, which is the x-axis in the 2D case. Then the second fitting goal can be written more specifically as follows:

$$\epsilon \left(\mathbf{D_x I_z m} - \delta\tau_{\mathbf{obs}}\right) \approx \mathbf{0} \tag{2}$$

where $\mathbf{I_z}$ is the vertical integration operator, $\mathbf{m}$ is the slowness (inverse of velocity),

$\mathbf{D_x}$ is the difference operator along the x axis, and is dimensionless; the other symbols are the same as in equation 1.

To update the velocity, I use the nonlinear conjugate gradient method. I first calculate the gradient of equation 1, and then I calculate the step length using a method similar to that proposed by Mora (1981).

SYNTHETIC EXAMPLE

I test the algorithm on a synthetic velocity example which is a modified version of the Amoco-Statics94 synthetic velocity model. To create the model, I first window out a small part of the whole velocity model, then retain some near-surface features and replace the deeper part of the velocity model with a constant velocity gradient plus a reflector (Figure 1a). An enlarged view of the near-surface part is shown in Figure 3a. I then compare the velocity-estimation algorithm with and without the RRSD constraint. I also compare the images produced by the two velocity-estimation methods.

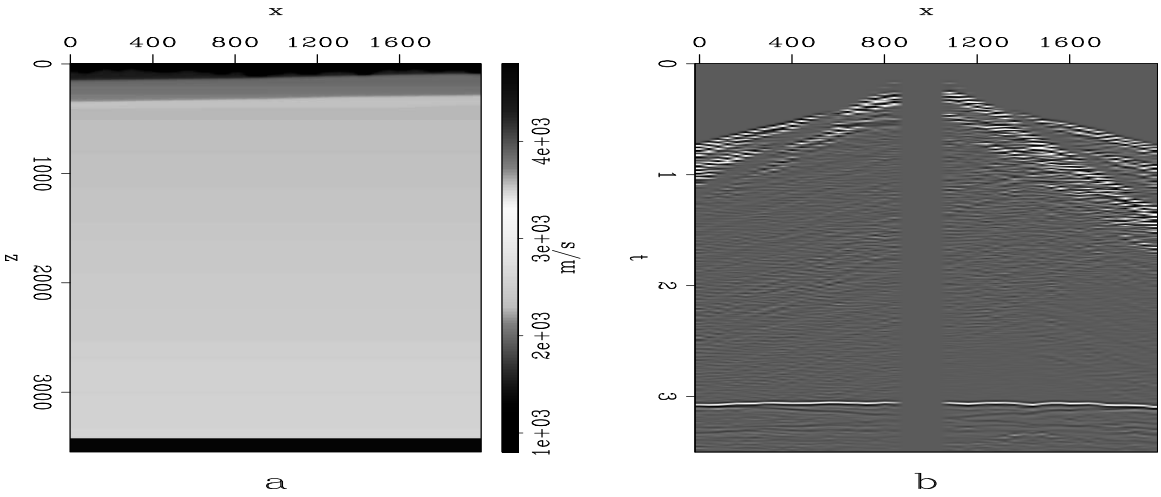

Figure 1: (a) The true velocity field with a 5 m spacing grid. (b) One typical synthetic shot record. [**CR**]

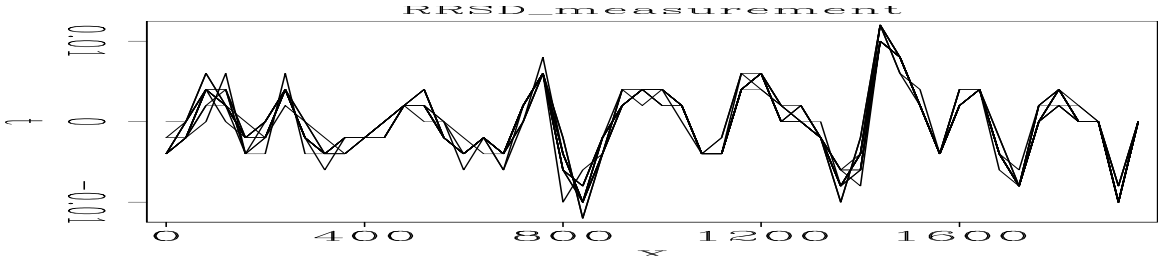

Figure 2: RRSD measured from all shot and receiver locations. [**CR**]

The major feature of the synthetic near-surface velocity model is a weathered layer with rapidly varying thickness. Immediately below this weathered layer, there is a reflector that gently dips upwards towards the right. Also notice that the velocity of the weathered layer gradually decreases from left to right. The deep reflector is located at about 3.2 km depth. The size of the velocity model is 2000 m in x and 3450 m in z with the spacing of both x and z being 5 m. I generate 15 synthetic shots from $x = 120$ m to $x = 1860$ m with 120 m shot spacing, using the first derivative of the Gaussian as the source wavelet. The peak frequency of the source wavelet is 25 Hz. The receiver spacing is 40 m with nearest offset of 100 m, and the recording time sampling is 2 ms. A typical shot is shown in Figure 1b. For the measured RRSD, the time sampling is 2 ms. RRSD measurements from all 15 shots are shown in Figure 2. Although measurements at the same receiver location from different shots are not the same, they follow approximately the same trend. For near-surface velocity estimation, the z and x spacings are both 10 m. The starting velocity model is a smooth version of the true near-surface velocity model (Figure 3a). I smooth it in such a way that the bottom of the weathered layer loses all details, and the dipping reflector below it follows the same shape as the smoothed bottom of the weathered layer and no longer dips to the right.

Influence of receiver sampling on velocity estimation result

As mentioned before, receiver spacing will affect the resolution of estimated velocity by early-arrival waveform inversion. Here I run the early-arrival waveform inversion without the RRSD constraints for two cases, one with receiver sampling of 10 m , the other with receiver sampling 40 m. The estimated near-surface velocity is shown in Figure 4. It can be seen that estimated velocity with receiver spacing of 10 m has higher resolution compared with the result using 40 m spacing receiver data.

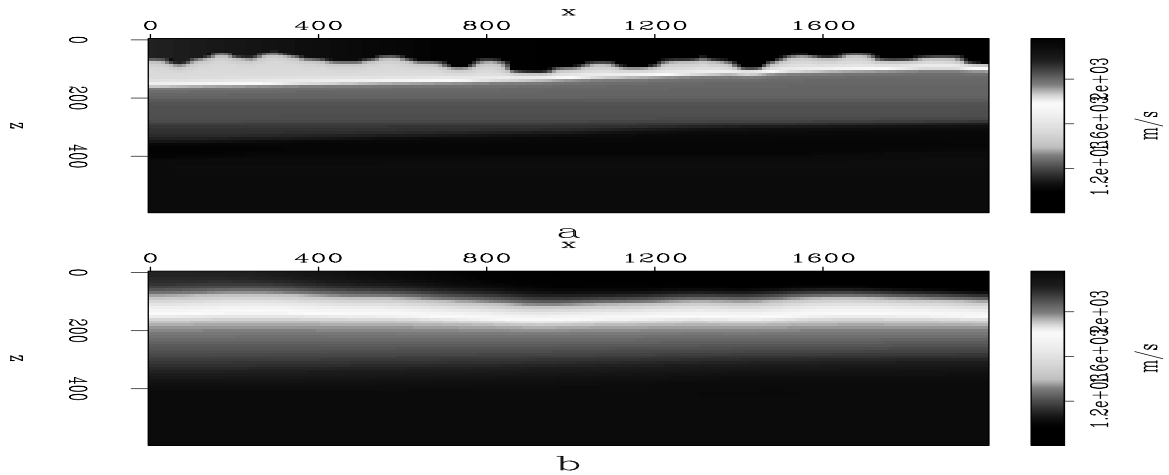

Figure 3: (a) The true near-surface velocity model with a 10 m spacing grid. (b) The starting velocity model for velocity estimation. [**CR**]

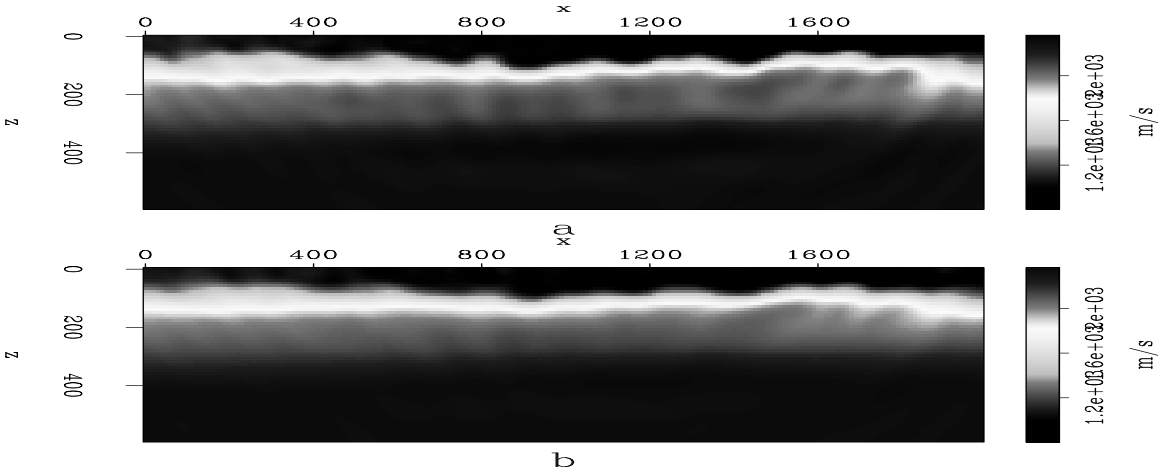

Figure 4: Early-arrival waveform inversion without RRSD using data recorded on different receiver spacing. (a) Estimated velocity with 10 m receiver spacing. (b) Estimated velocity with 40 m receiver spacing. [**CR**]

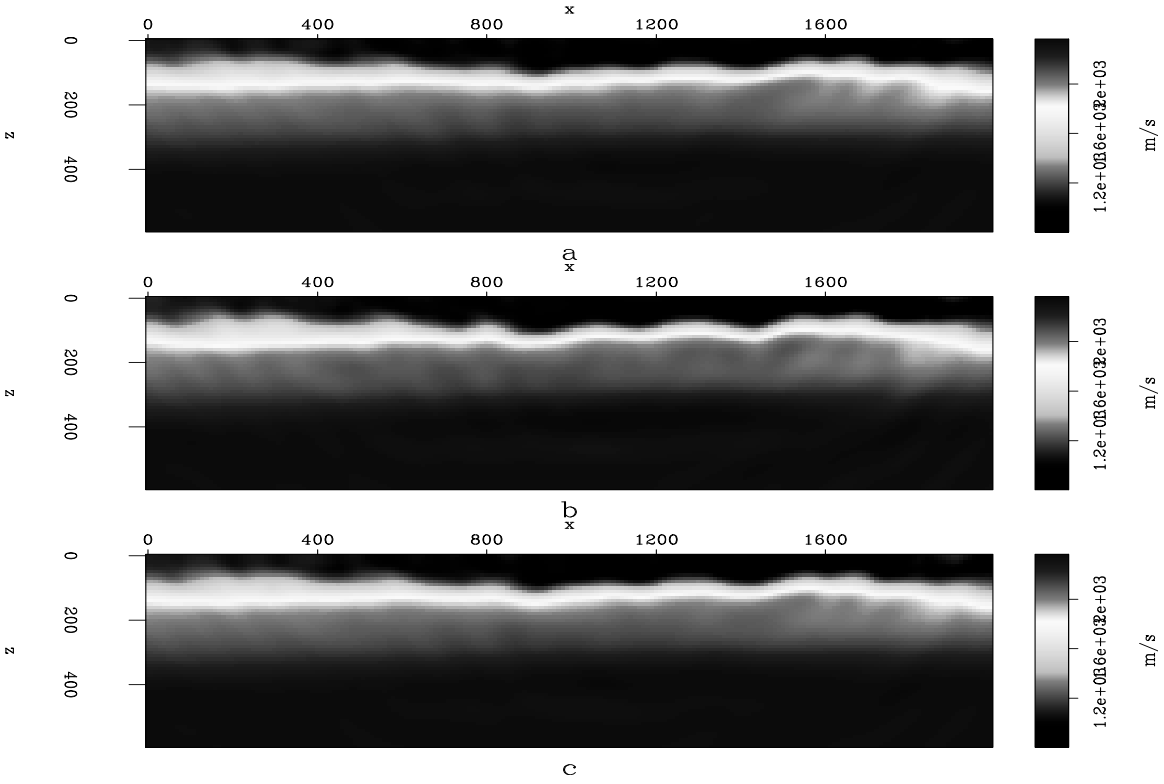

Figure 5: (a) Estimated velocity without RRSD constraints. (b) Estimated velocity with RRSD constraints. (c) Estimated velocity with starting model improved by RRSD constraints alone [**CR**]

RRSD constrained velocity estimation result

To simulate more realistic settings, I use data recorded on 40 m receiver spacing in this synthetic example. From the starting model, I estimate the velocity by three variations of the alogrithm. In the first variation, I apply the algorithm without the RRSD constraints using early arrivals from 6 Hz to 10 Hz to obtain a velocity model that is closer to the true velocity model, then I use early arrivals from 9 Hz to 14 Hz to estimate the velocity also without RRSD constraints. The final estimated velocity for this case is shown in Figure 5a. For the second variation, the first step is the same as that of the first variation, in the second step, I use early arrivals from 9 Hz to 14 Hz to estimate the velocity with RRSD constraints. The final estimated velocity for this case is shown is Figure 5b. For the third variation, I first use the RRSD constraints alone to estimate a velocity field from the starting model, then I follow the same two step method in the first variation. The final result for this case is shown in 5c. It can be seen that with RRSD constraints, the estimated velocity has more sharply defined layer boundaries, and the reflector immediately below the bottom of the weathered layer is more correctly positioned, while using velocity estimated by the RRSD constraints alone for the following early-arrival waveform inversion results in an estimated velocity that is almost the same as using early-arrival waveform inversion on the original starting model. The starting residual early arrivals and the final residual early arrivals for the second pass of case one, case two and case three are shown in Figure 6, Figure 8 and Figure 7, respectively. Also, the RMS early-arrivals residual for the three variations is shown in Figure 9. Notice that both the early-arrival residual and its RMS are consistently smaller in the case of velocity estimation with RRSD constraints, while they are almost the same for the other two variations. Another way to say this is that the RRSD constraints help to speed the convergence of the velocity-estimation process, while the starting model derived by RRSD constrains alone does not result in much improvements in the final estimated velocity.

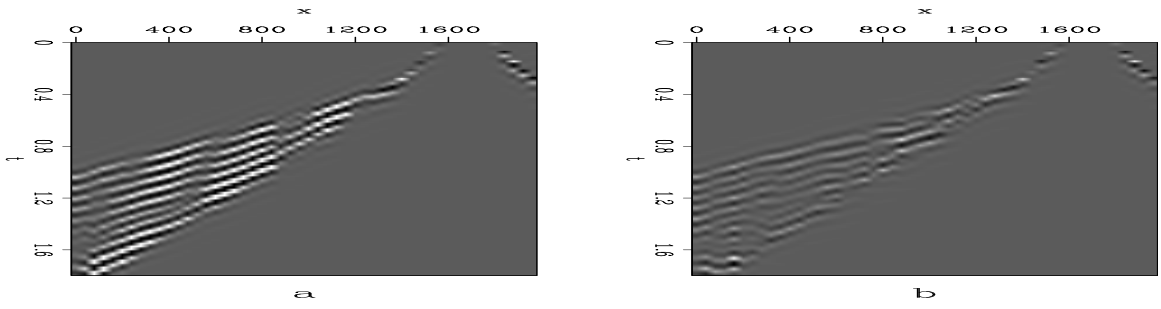

Figure 6: Early-arrival residuals for velocity estimation without RRSD; both panels are clipped to the same value. (a) Starting residuals. (b) Final residuals. [**CR**]

Next, I compare the migrated images using these three velocities. All the images shown include only the part containing the deep reflector, since this is usually the area of interest. First I migrate each individual shot, and put all 15 images into a cube, to see if the reflector is consistently at the same depth (Figure 10). It can be seen

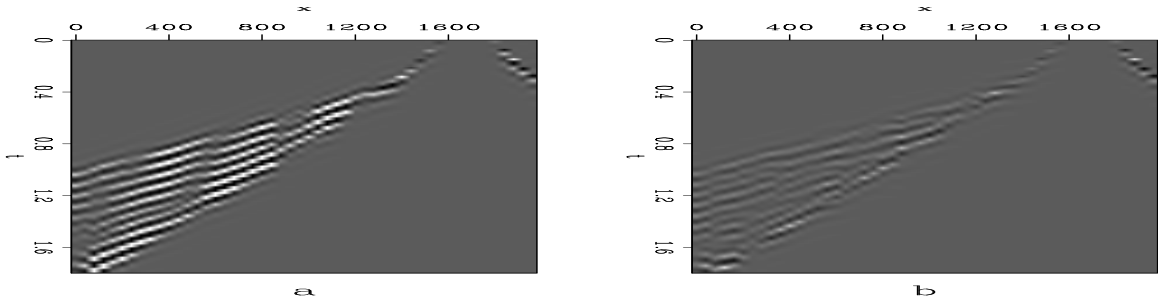

Figure 7: Early-arrival residuals for velocity estimation with RRSD; both panels are clipped to the same value. (a) Starting residuals. (b) Final residuals. [**CR**]

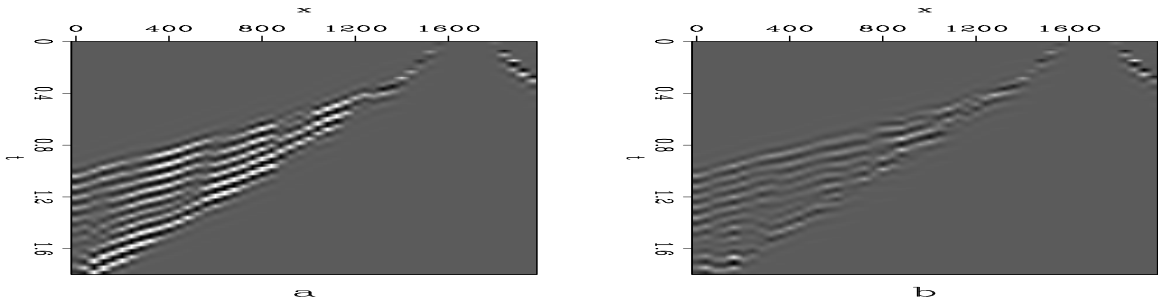

Figure 8: Early-arrival residuals for velocity estimation with starting model improved by RRSD constraints alone; both panels are clipped to the same value. (a) Starting residuals. (b) Final residuals. [**CR**]

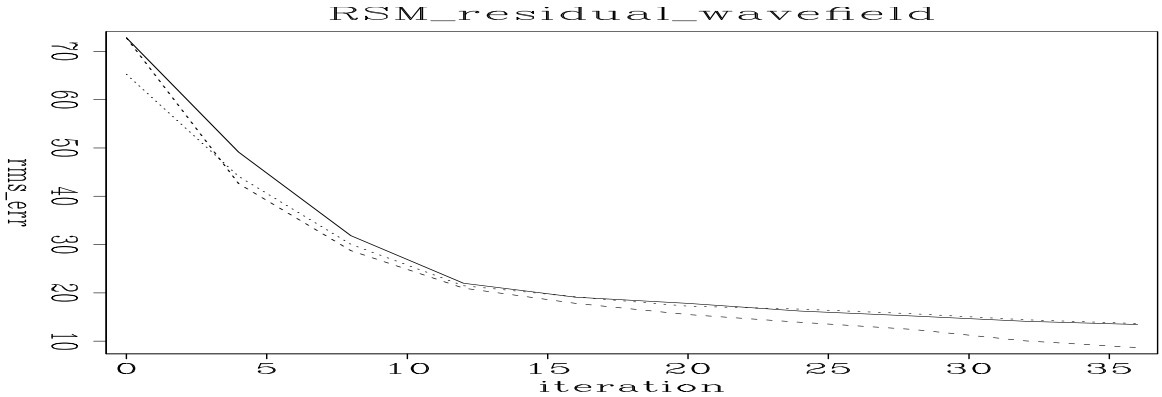

Figure 9: Change of RMS early-arrival residuals as a function of iteration. Solid curve is for estimation without RRSD, dashed curve is for estimation with RRSD, dotted curve is for estimation with starting model improved by RRSD constraints alone. [**CR**]

that for migrated images using the velocity estimated without RRSD constraints, the reflector in different images is not consistently at the same depth. However, in the images using the velocity estimated *with* RRSD, the reflector depth is more consistent across different images. While the images using the estimated velocity with starting model improved by RRSD constraints alone is almost the same as 10b. When I stack all the images together (Figure 11), images using velocity estimated with RRSD constraints are slightly more continuous laterally since the reflector from images of different shots are more consistently positioned . Thus migrated images using estimated velocity from RRSD are more consistent in depth.

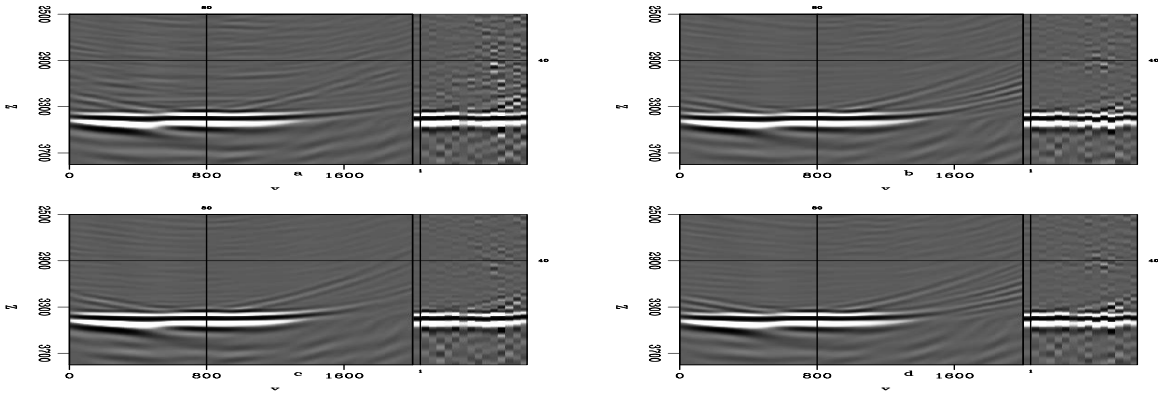

Figure 10: Migrated images of all 15 shots, showing only the deeper part with the reflector. Front panels are images of one shot. Right panels are images at the same x location from different shots. Top panels are constant depth image from different shots. (a) Migrated with true near-surface velocity model. (b) Migrated with estimated velocity without RRSD constraints; notice that different shots do not put the reflector at the same depth. (c) Migrated with estimated velocity with RRSD constraints. Notice in this case the reflector depth is almost the same as that migrated with the true velocity. (d) Migrated with estimated velocity with starting model improved by RRSD constraints alone.[**CR**]

CONCLUSIONS

In the synthetic example, near-surface velocity estimation with RRSD results in a velocity estimate with higher resolution and faster convergence. Also the migrated images have deep reflectors more consistently positioned at the same depth. The algorithm still needs to be tested on real land data before more general conclusions can be made. For real data, the noise will more strongly bias the RRSD measurement, in which case, using the L1 norm in the RRSD constraint might work better. Also, this algorithm works only in places where near-surface velocities are slower than the deeper velocities. In these places, near-surface velocity is slower compared with deeper velocities so the vertically traveling rays assumption is valid. Therefore, when near-surface velocity is higher (e.g. in permafrost), this method is unlikely to work. Then angle-dependent residual statics (Henley, 2009) can potentially better define

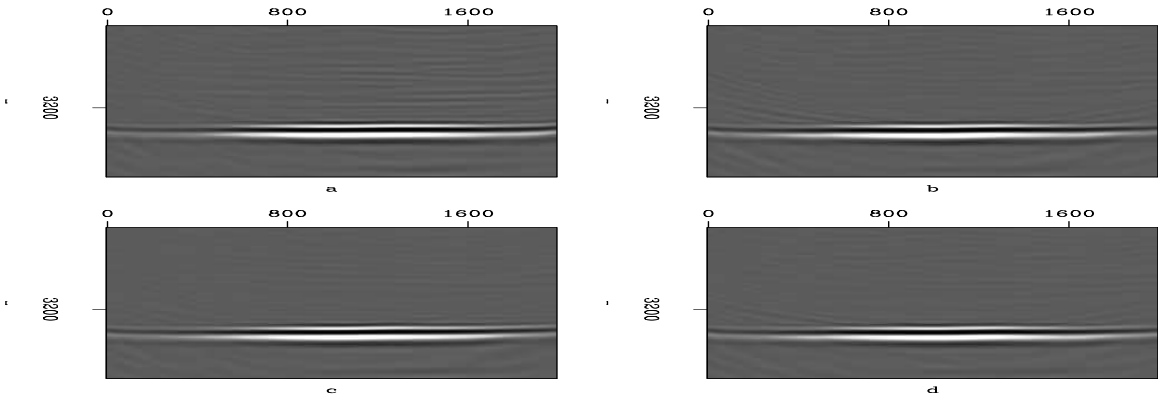

Figure 11: Stack of images from all shots, all are clipped to the same value. (a) Migrated with true velocity. (b) Migrated with estimated velocity without RRSD; notice that the reflector is of lower frequency content due to stacking of reflectors from different shots that are not at the exact same depth . (c) Migrated with estimated velocity with RRSD; notice that this image is almost identical to the image migrated with true velocity. (d) Migrated with estimated velocity using starting model improved by RRSD constraints alone.[**CR**]

the ray path of reflection events and be used to connect near-surface velocity with such residual statics.

ACKNOWLEDGMENTS

I would like to thank Biondo Biondi, Shuki Ronen, Robert Clapp, Antoine Guitton and Jon Claerbout for a lot of helpful suggestions and discussions.

REFERENCES

C. Ravaut, S. Operto, L. I. J. V. A. H. and P. Dell'Aversana, 2004, Multiscale imaging of complex structures from multifold wide-aperture seismic data by frequency-domain full-waveform tomography: application to a thrust belt: Geophysical Journal International, **159**, 1032–1056.

Hampson, D. and B. Russell, 1984, First-break interpretation using generalized linear inversion: Journal of CSEG, **20**, 40–54.

Henley, D. C., 2009, Raypath interferometry: Statics in difficult places: The Leading Edge, **28**, 202–205.

J. Sheng, A. Leeds, M. B. and G. T. Schuster, 2006, Early arrival waveform tomography on near-surface refraction data: Geophysics, **71**, U47–U57.

Mora, P., 1987, Elastic wavefield inversion: SEP Ph.D Thesis.

Olson, K. B., 1984, A stable and flexible procedure for the inverse modelling of seismic first arrivals: Geophysical Prospecting, **37**, 455–465.

Pratt, R. G., S. C. and G. Hicks, 1998, Gauss-Newton and full Newton methods in frequency domain seismic waveform inversion: Geophysical Journal International, **133**, 341–362.

Ronen, J. and J. F. Claerbout, 1985, Surface-consistent residual statics estimation by stack-power maximization: SEP report 42.

Rothman, D. H., 1985, Automatic estimation of very large residual statics: SEP report 42.

Sirgue, L. and R. G. Pratt, 2004, Efficient waveform inversion and imaging: A strategy for selecting temporal frquencies: Geophysics, **69**, 231–248.

Tarantola, A., 1984, Inversion of seismic reflection data in the acoustic approximation: Geophysics, **49**, 1259–1266.

White, D. J., 1989, Two-dimensional seismic refraction tomogaphy: Geophysical Journal International, **97**, 223–245.